RSC Advances

RSC Advances

www.rsc.org/advances

ROYAL SOCIETY OF CHEMISTRY

www.rsc.org/advances

Three independent channels nanohybrids as fluorescent probes

Soranyel Gonzalez-Carrero, Carlos Agudelo-Morales, Miguel de la Guardia, Raquel E. Galian,*
and Julia Pérez-Prieto*

Pyrene-capped CdSe/ZnS nanohybrids permit a simple and rapid quantification of trinitrotoluene in the presence of interferents of the same chemical family.
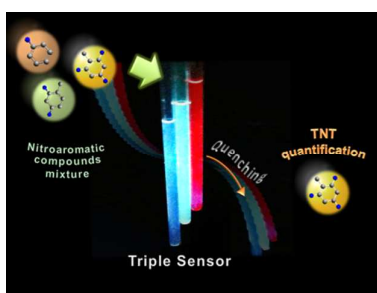
Journal Name

ARTICLE

Three independent channels nanohybrids as fluorescent probes

Soranyel Gonzalez-Carrero,[a] Carlos Agudelo-Morales,[a] Miguel de la Guardia,[b] Raquel E. Galian,[a]* and Julia Pérez-Prieto [a]*

A properly designed pyrene-capped CdSe/ZnS nanohybrid can act as a three-channel fluorescence sensor due to its independent emission of the pyrene monomer and excimer as well as that of the nanoparticle. As proof of principle, it was tested for a simple and rapid quantification of TNT in the presence of interferents of the same chemical family.

Introduction

Fluorescence sensing is a powerful strategy to detect molecular targets and it is consequently a widely-used technique in chemistry, biology, and medicine.[1-3] Though a huge number of fluorescent probes have been developed, most of them exhibit fluorescence signal variations in only one channel.[4] Multi-channel based probes can be highly useful for i) reducing errors due to false positives and interferents, ii) providing simultaneous detection, and even quantification, of analytes of a dissimilar structure and/or closely related structures, among other applications. There are considerably fewer examples of two-channel probes,[5, 6] and probes able to detect chemical species in three different emissive channels (single excitation/triple channel emission) are uncommon.[7, 8] Moreover, if those channels were independent channels it would be even more advantageous, but to our knowledge this has not been reported yet. In fact, we recently reported the preparation of pyrene-capped core-shell CdSe/ZnS quantum dots (CS@Py) which present three fluorescent channels: i) the Py monomer (M*), ii) the Py excimer (E*),[9,10, 11] and iii) the nanoparticle excited state (CS*).[12] These nanohybrids were tested as sensors of the oxygen concentration, $[O_2]$, in organic solvents. However, the channels failed to give a linear response to the analyte due to the fact that the solubility of $[O_2]$ in the solvents is high, as well as being due to the formation of complexes between the analyte and the pyrene channel.

We then realised that CS@Py (Figure 1) could be suitable as three independent channel fluorescent probes provided that there was a low concentration of the analyte, which is usually

the aim of a sensor, i.e., to be able to detect the least amount of the analyte as possible. As proof of concept, we chose nitroaromatic compounds (NACs, Figure 1) as highly challenging test of the performance of these nanohybrids, since i) NACs quench both the M* and E* of Py-capped NPs and the decrease of E* emission hardly reflects the quenching of M*, i.e., the E* and M* emissive channels would behave as independent channels[13]; ii) CS@Py are highly emissive and the size of the core of the CS avoids the overlap between its specific emission and those of M* and E*; iii) trinitrotoluene (TNT) is a relevant explosive and other NACs, in particular 2,4-, and 2,6-dinitrotoluene (2,4-DNT, and 2,6-DNT, respectively) are TNT by-products.

Different techniques have been used to detect NACs, such as gas chromatography coupled with mass spectroscopy, X-ray imaging, surface enhanced Raman spectroscopy, micro-fabricated gas chromatography, among others.[14] Fluorescence has proved to be a highly competitive technique (high sensitivity, simple operation, and uses cost-effective instrumentation).[15-17] Several materials have been used as fluorescent probes, such as conjugated polymers,[18] self-

[a.] Instituto de Ciencia Molecular (ICmol), Universidad de Valencia, Catedrático José Beltrán 2, 46980, Paterna, Valencia, Spain. Fax: 34 963543576; Tel:34963543050; E-mail: raquel.galian@uv.es, julia.perez@uv.es
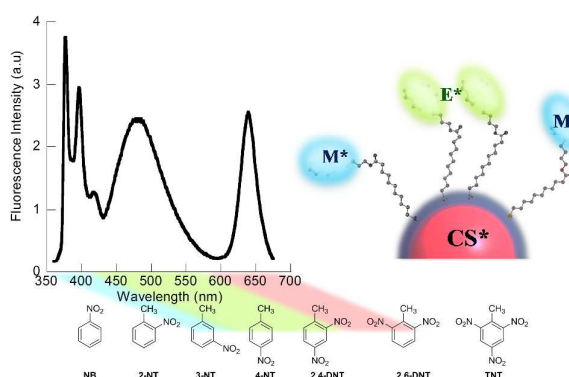[b.] Depart. Química Analítica, Univ. de Valencia, Dr. Moliner 50, Burjassot, 46100, Valencia, Spain.

Figure1: Fluorescence spectrum (λexc= 340 nm) of CS@Py (64 nM) in THF. Schematic picture of the three emissive species: M* (397 nm), E* (480 nm), and CS* (640 nm) of CS@Py. Structure of the tested nitroaromatic compounds (NACs).

COMMUNICATION

assembly molecular gelators,[19] metal organic frameworks, [20] and hybrid organic-inorganic materials.[21]

We demonstrate here that CS@Py nanohybrids are unique systems since they can act as probes with three independent fluorescent channels. Thus, NACs (nitrobenzene, NT; 2-nitrotoluene, 2NT; 3-nitrotoluene, 3NT; 4-nitrotoluene, 4NT; 2,4DNT; 2,6DNT and 2,4,6-trinitrotoluene, TNT (Figure 1) proved to be efficient quenchers, by decreasing the intensity of the three channels independently. As proof of the applicability of this smart nanohybrid, we focussed our efforts on developing a simple, rapid, and inexpensive method for quantifying TNT in binary and ternary mixtures of NACs, based on their different capacities as quenchers of the fluorescence intensity of the three emissive species (M*, E*, and CS*).

Experimental section

Reagents and techniques

All reagents were commercially available and used as received. The 11-mercaptoundecanol (MU), and 1-pyrenebutanol were purchased from Sigma-Aldrich. Toluene and tetrahydrofuran of HPLC grade were purchased from Scharlau. The core shell (CS) capped with long-chain primary amine was purchased from Ocean Nanotech LLC. The NCs were purchased from Sigma-Aldrich, except for TNT, which was synthesized.

UV-Vis spectra of the samples were recorded using a quartz cuvettes spectrometer in a UV-visible spectrophotometer Agilent 8453E. Steady-state fluorescence spectra (LPS-220B, motor driver MD-5020, Brytebox PTI) were measured on a spectrofluorimeter PTI, equipped with a lamp power supply and working at room temperature. The Felix 32 Analysis software was used to register the data. All the data were acquired using 1cm×1cm path length quartz cuvettes

Time-resolved measurements were made with a Time Master Fluorescence lifetime spectrometer TM-2/2003 from PTI. Sample excitation was afforded by PTI's own GL-3300 nitrogen laser. The kinetic traces were fitted by mono- or biexponential decay functions and deconvolution of the instrument response function. The accuracy of the fits was evaluated by the reduced χ^2 values ($0.8 > \chi^2 < F\ 1.2$).

CS nanoparticles images were obtained by high-resolution transmission electron microscopy (HRTEM, FEI Tecnai G2 F20) at an accelerating voltage of 200 kV. Samples were prepared by dropping the colloidal solution on a Lacey Formvar/carbon-coated copper grid. The digital analysis of the HRTEM micrographs was done using digital MicrographTM 1.80.70 for GMS by GATAN.

^{1}H-NMR (CDCl$_3$) spectra were recorded on 300 MHz spectrometrer (Bruker AVANCE DRX 300). The samples were dissolved in deuterated chloroform.

Synthesis of the nanohybrid CS@Py

The CS@Py was synthesized following the previous described methodology.[12] The CS@Py concentration of a sample was determined by first estimating the average diameter value of the CdSe core (exciton peak at 622 nm) and then estimating

the extinction coefficient at the exciton peak wavelength (see Peng et al[22] equation). The number of Py units on each nanoparticle was estimated by firstly determining the extinction coefficient of Py in THF (ε=13193 M^{-1}cm^{-1}). The absorbance at 335 nm of a solution of CS@Py and that of CS, both at the same nanoparticle concentration, were registered. The difference between these absorbances was attributed to Py (A$_{Py}$(335 nm)=A$_{CS@Py}$-A$_{CS}$), thus allowing the estimation of Py concentration [Py]=A$_{Py}$(335 nm)/εb, and, eventually, the ratio of Py units per nanoparticle.

The quantification of the organic capping of the hybrid nanoparticles (CS@Py) has been carried out by combining the absorption and the NMR techniques. The ^{1}H-NMR spectra of CS@Py and the thiol ligand (Py-SH) were recorded in deuterated chloroform and they were compared with that of CS in the same solvent. The more significant signals of the aliphatic chain of the Py-SH and that of the amine of CS were used to identify and quantify the total Py-SH (bonded and free) and the remaining amine on the CS@Py nanohybrid.

3. Results and Discussion

Properties of the fluorescent probe

The nanohybrid[12] was prepared from a commercial amine-capped CS (λ_{abs}= 622 nm, λ_{em}= 640 nm, with a total and core diameter of 8.7 ± 1.5 nm and 5.8 nm, respectively, and with a fluorescence quantum yield, Φ_f, of 0.38), by means of a ligand exchange strategy with a pyrene derivative possessing a long flexible chain ending in a thiol group to anchor the CS surface (Py-SH).[23] Transmission electron microscopy (TEM) images of CS@Py demonstrated that the CS crystallinity and size remained after functionalization (Figure S1). The molar extinction coefficient (ε) of the nanoparticle was estimated as 6.14 x 10^5 M^{-1}cm^{-1}. [22] The photophysical properties of the CS@Py are summarised in Table S1 in ESI.

The absorption spectrum of CS@Py in tetrahydrofuran (THF) showed a small exciton peak at 622 nm and well-resolved peaks below 350 nm corresponding to the Py units (Figure 2).
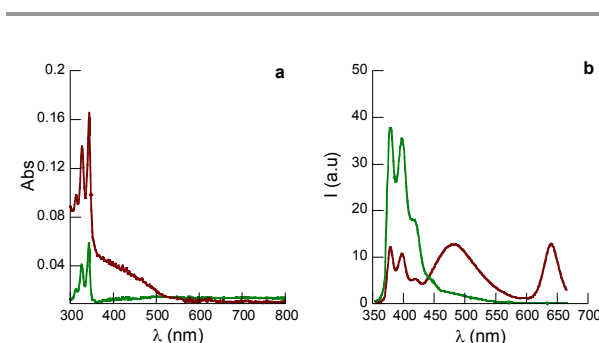

Figure 2: a) absorption and b) fluorescence (λ_{exc}= 340 nm) spectra of CS@Py (5 nM, garnet) and PySH (1 µM, in green) in THF; both with the same pyrene concentration (1 µM).

The average number of Py moieties was calculated to be ca. 200 per nanoparticle taking into account the average size of the nanoparticles. Absorption and nuclear magnetic resonance (NMR) spectroscopy were used to determine the Py number. Thus, the pyrene contribution to the absorbance at 335 nm of a THF solution of CS@Py was estimated by using the molar absorption coefficient of pyrene (13193 $M^{-1} cm^{-1}$ in THF). The ^{1}H-NMR spectrum of CS@Py mainly showed broad peaks due to the restricted motion of the surface ligands. Quantification of the components revealed that the ligand exchange was not complete (88:12 tiol/amine molar ratio) and that free PySH was less than 1%.

The fluorescence spectrum of CS@Py (Figure 2) presented the emission bands corresponding to the three emissive species i) M* at ~ 370 nm, 397 nm, and ~ 420 nm, ii) E* centred at 480 nm, and iii) CS* at 640 nm. The high local concentration of Py at the CS periphery enabled formation of E* in an otherwise diluted solution (μM concentration). It should be taken into account that E* is not efficiently formed at μM concentrations (Figure 2), therefore the E* formation is due to a synergetic effect between the organic capping and the nanoparticle.[24] The CS@Py nanohybrid exhibited a lower Φ_f than the amine-capped CS (21% vs 38%).

Time-resolved measurements showed that the average fluorescence lifetime (τ_{av}) of the CS remained almost the same after Py-functionalization. Therefore, in view of equation 1, where k_r is the radiative constant, the functionalization caused a decrease in k_r of ca. 40% (from 9.80×10^6 s^{-1} to 5.95×10^6 s^{-1}); this is consistent with the reported effect of sulphur atoms slowing down the radiative process.[25] By using equation 2, the non-radiative (k_{nr}) constant was calculated, and showed that the ligand exchange caused an increase in k_{nr} (from 16.2×10^6 s^{-1} to 22.4×10^6 s^{-1}). This behaviour is consistent with the alteration of the QD surface caused by the thiolate binding,[26] thus making the electron density locate at shallow trap states close to the conduction band edge.[25] With regard to the pyrene species of CS@Py, M* exhibited two components at 87.4 and 15.9 ns (Figure S2). The short decay lifetime coincided with the growth lifetime of E* (17.3 ns) as has been previously observed for CdSe@Py.[13] Comparatively, under the same conditions, pyrene exhibits one component with a lifetime of 94.7 ns.

$$\phi_F = \tau_{av} \times k_r \quad \text{Equation 1}$$

$$\tau_{av} = \frac{1}{k_r + k_{nr}} \quad \text{Equation 2}$$

Figure 3 shows the evolution of the CS@Py fluorescence spectrum recorded at different times after excitation at 337 nm (nitrogen laser). The highest intensity of E* was found after 35 ns of the laser pulse.
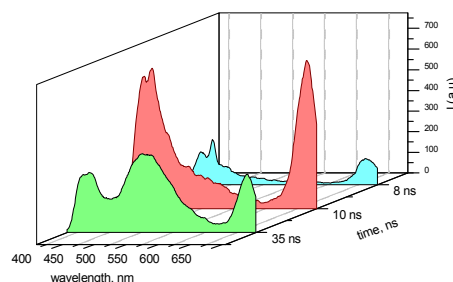

Figure 3: Fluorescence spectra of CS@Py in THF at different times (8, 10 and 35 ns) after the laser pulse (337 nm).

Steady-state and time-resolved fluorescence quenching studies

The variation of the fluorescence intensity and lifetime in the presence of increasing amounts of the NAC was recorded for the three emissive channels to determine the nature and efficiency of the quenching processes. The NAC concentration was kept under 0.25 mM and the emission intensities were corrected for the primary and secondary filter effects due to the absorbance of the NAC at the excitation and emission wavelengths, respectively. See Figure 4 for TNT analyte and Figure S3 and S4 for the other compounds.[27, 28]

Both the emission intensity and lifetime of the three channels showed a linear dependence on the NAC concentration (see Figure 5 for TNT and Figures S6 for all the NACs). The corresponding quenching constants (K_{sv} and K_d) were calculated by using Stern-Volmer equations 3 and 4.
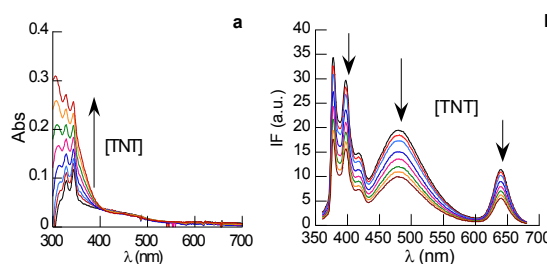

Figure 4: a) absorption and b) emission spectra (λexc= 340 nm) of CS@Py (5 nM) at different concentration of the NAC (0-0.25 mM) in THF, under N2 atmosphere.
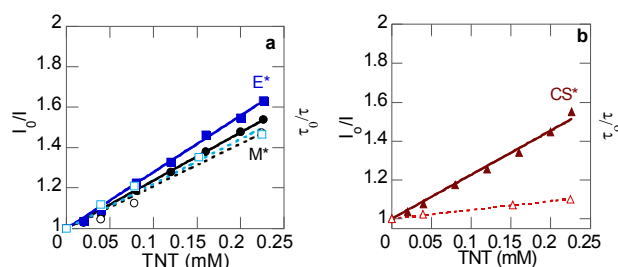

Figure 5: Stern-Volmer plots showing the intensity (▬), and lifetime (----) dependence of M*, E*, and CS* emission of CS@Py (5 nM in THF, λ_{exc} = 340 nm) on TNT concentration.

$$\frac{I_0}{I} = 1 + K_{SV}.[Q] \qquad \text{Equation 3}$$

$$\frac{\tau_0}{\tau} = 1 + K_d.[Q] \qquad \text{Equation 4}$$

The quenching of the Py species is mainly of a dynamic nature as shows the similarity between the values of K_{sv} and K_d (see Table 1 for K_{sv} and Table S2 for K_d). However, in the case of the CS, the quenching is mainly static for all the NACs, but in NB the quenching is exclusively static. These data are consistent with some NAC encapsulation within the organic capping and therefore close to the CS surface and also near to the Py units. This is another manifestation of the synergetic effect between the organic and inorganic components of the nanoparticle.[24]

The sensitivity of each individual channel towards the NACs was analysed by using the K_{sv} values. The values decreased in the following order i) 2,6DNT > TNT > 4NT ~ 3NT > 2NT > 2,4DNT ~ NB for M* channel; ii) 4NT~TNT ~ 2,6DNT > NB > 3NT> 2NT > 2,4DNT for the E* channel, and iii) TNT > 2,6DNT > 2NT > 3NT ~ 2,4DNT > 4NT > NB for the CS* channel.

The limit of detection (LOD) and quantification (LOQ) were calculated using the IUPAC criteria, based on the sensitivity and three and ten times the blank measurement standard deviation for LOD and LOQ, respectively.

The LOD values were under 0.13 ppm, while LOQ values were under 0.32 ppm (Table 2). Consequently, all the NACs were suitable to be quantitatively determined at trace levels.

Table 1 Stern-Volmer quenching constants (k_{sv}) of the pyrene monomer, M*, pyrene excimer, E*, and nanoparticle excited state (CS*) in the CS@Py hybrid by the nitroaromatic compounds

NAC	$K_{sv}{}^a$		
	M*	E*	CS*
NB	1197 ± 45 (0.992)	1995 ± 74 (0.992)	753 ± 21 (0.995)
2NT	1572 ± 31 (0.995)	1627 ± 28 (0.996)	1457 ± 23 (0.997)
3NT	2078 ± 50 (0.996)	1804 ± 33 (0.997)	1248 ± 37 (0.993)
4NT	2160 ± 82 (0.994)	2805 ± 76 (0.997)	1049 ± 63 (0.989)
2,4 DNT	1220 ± 53 (0.991)	1306 ± 45 (0.990)	1200 ± 53 (0.991)
2,6 DNT	2848 ± 160 (0.986)	2672 ± 188 (0.980)	1963 ± 60 (0.996)
TNT	2372 ± 32 (0.998)	2786 ± 34 (0.999)	2267 ± 50 (0.995)

a Ksv units: M-1; data obtained from the steady-state measurements.

Table 2 Calculated LOD and LOQ for the determination of the nitroaromatics compounds considered using the three channels CS@Py

NAC	M*		E*		CS*	
	LOD (ppm)	LOQ (ppm)	LOD (ppm)	LOQ (ppm)	LOD (ppm)	LOQ (ppm)
NB	0.09	0.29	0.04	0.14	0.06	0.21
2NT	0.07	0.24	0.06	0.19	0.03	0.12
3NT	0.06	0.18	0.05	0.17	0.04	0.14
4NT	0.05	0.18	0.03	0.11	0.05	0.15
2,4 DNT	0.13	0.42	0.10	0.32	0.06	0.19
2,6 DNT	0.05	0.18	0.05	0.16	0.04	0.12
TNT	0.08	0.27	0.06	0.19	0.04	0.13

Quantification of TNT in binary and ternary mixtures of NACs

The performance of CS@Py as a three independent channel, fluorescent probes was evaluated for the TNT quantification in binary and ternary mixtures.

The proportional equations approach provided quantitative data about TNT, NB, and 3NT mixtures by using, at least, the same number of independent equations than target analytes.

The variation of the fluorescence intensity (I_0/I) in the system and the concentration of the NACs follow, in the steady-state, equation 5, where K_{NAC} is the Stern-Volmer quenching constant and C_{NAC} is the concentration of each of the NACs in the sample.

$$\frac{I_0}{I} = \Sigma K_{NAC}.C_{NAC} \quad \text{Equation 5}$$

Table 3 shows the data obtained for TNT/NB and TNT/3NT binary mixtures at 0.5:1 and 1:1 molar ratios, respectively, and a TNT concentration of 0.150 mM. The relative error (E%) between the theoretical and calculated TNT concentrations varied from 1.4 to 24.1% depending on the system, the relative concentration of the compounds, and the channels selected for the data treatment. So being confirmed that TNT and NB or mixtures of TNT and 3NT can be accurately analysed based on the proper selection of channels, being found the best results using M* and CS* channels and E* and CS* channels, respectively.

For TNT quantification in the presence of NB, the use of the monomer channel provided the lowest accuracy errors (1.4 and 2.9% at 0.5:1 and 1:1 molar ratios, respectively) as a function of the proportion between these compounds. However, in the presence 3NT, the minimum errors found for TNT quantification were 6.4 and 8.6 % using the excimer channel.

COMMUNICATION

Table 3 Quantification of TNT in TNT/NB and TNT/3NT binary mixtures

	Calculated concentration (mM)			
	C_{TNT}/C_{NB} 1:0.5 molar ratio [a]		C_{TNT}/C_{NB} 1:1 molar ratio [b]	
	C_{TNT} (E %)	C_{NB} (E %)	C_{TNT} (E %)	C_{NB} (E %)
M*	0.148 (1.4)	0.073 (5.4)	0.145 (2.9)	0.139 (5.8)
E*	0.145 (3.3)	0.070 (8.2)	0.131(11.6)	0.126 (14.6)
CS*	0.148 (1.3)	0.072 (6.6)	0.140 (5.1)	0.128 (13.5)
	Calculated concentration (mM)			
	C_{TNT}/C_{3NT} =1:0.5 molar ratio [a]		C_{TNT}/C_{3NT} =1:1 molar ratio [b]	
	C_{TNT} (E %)	C_{3NT} (E %)	C_{TNT} (E %)	C_{3NT} (E %)
M*	0.119 (21.1)	0.047 (38.0)	0.112 (24.1)	0.108 (26.7)
E*	0.141(6.4)	0.062 (17.1)	0.161 (8.6)	0.165 (12.0)
CS*	0.131 (12.7)	0.044 (41.4)	0.138 (6.4)	0.132 (10.0)

[a]Theoretical concentration: 0.150 mM (TNT) and 0.077 mM (NB and 3NT). [b]Theoretical concentration: 0.148 mM for TNT, NB, and 3NT. The E% is the ratio of the absolute error of the measurement (i.e., the difference between measured value and the actual value) to the actual value multiply by 100.

Table 4 and table S4 show the data for TNT/NB/3NT and TNT/NB/2,4DNT ternary mixtures, respectively. The errors in the quantification of TNT varied from 2.3 to 15%, but errors increase for the other nitrocompounds.

The aforementioned error can be considered as a good accuracy level for TNT quantification taking into account the closely related structures and the similarity of the quenching constants for the different analytes. This is possible due to the fact that the CS@Py nanohybrid provides information via three independent fluorescent channels. In short, for ternary mixtures of TNT, NB, and 3NT, the lowest accuracy errors, corresponding to the nanoparticle channel, were 2.6 and 9.0% as a function of the increase of the proportion of interferents. So, this clearly shows the tremendous flexibility of the CS@Py nanohybrid.

The proposed approach is a fast and simple method for TNT quantification in mixtures and could be an alternative to currently used methodologies.[29,30] Moreover, though not used in this TNT quantification, the data arising from the time-resolved studies, i.e., K_d values, could be used to provide additional equations or they could be combined with those of K_{sv} for the analysis of additional nitrocompounds species.

Table 4 Quantification of TNT in TNT/NB/3NT ternary mixtures

	Calculated concentration (mM)					
	CTNT/CNB/C3NT 1:0.5:0.5 molar ratio [a]			CTNT/CNB/ C3NT 1:1:1 molar ratio [b]		
	C TNT (E %)	CNB (E %)	C3NT (E %)	C TNT (E %)	CNB (E %)	C3NT (E %)
M*	0.071 (6.6)	0.029 (26.3)	0.031 (19.8)	0.065 (11.1)	0.06 (21.2)	0.068 (11.5)
E*	0.083 (6.8)	0.047 (21.0)	0.046 (18.3)	0.065 (10.7)	0.07 (15.7)	0.067 (14.0)
CS*	0.080 (2.6)	0.044 (14.2)	0.042 (8.7)	0.066 (9.0)	0.06 (22.6)	0.067 (14.0)

[a] Theoretical concentration: 0.076 mM (TNT) and 0.039 mM (NB and 3NT). [b]Theoretical concentration: 0.073 mM (TNT) and 0.077 mM (NB and 3NT). The E% is the ratio of the absolute error of the measurement (i.e., the difference between measured value and the actual value) to the actual value multiply by 100.

Conclusion

In summary, we report for the first time that CS@Py can be used as a fluorescent probe with three independent channels (single excitation/triple emission) and that it can be applied for analysing mixtures of compounds that can even have very similar structures and quenching efficiencies, by just using the variation in the fluorescence intensity of the three channels.. Nevertheless, fluorescence lifetimes can double the information and thus further enhance the versatility of the nanohybrid in sensing. The strategy herein described for building a three-channel emissive probe could also be applied to design other nanohybrids by using emissive nanoparticles capped with organic chromophores able to generate excimers and exciplexes at the nanoparticle periphery.

Acknowledgement

Notes and references

1. T. Liu, X. Liu, D. R. Spring, X. Qian, J. Cui and Z. Xu, *Scientific Reports*, 2014, **4**, 5418.
2. Y. Yang, Q. Zhao, W. Feng and F. Li, *Chemical Reviews*, 2013, **113**, 192-270.
3. T. Minami, N. A. Esipenko, A. Akdeniz, B. Zhang, L. Isaacs and P. Anzenbacher, *Journal of the American Chemical Society*, 2013, **135**, 15238-15243.
4. Z. Yang, J. Cao, Y. He, J. H. Yang, T. Kim, X. Peng and J. S. Kim, *Chemical Society Reviews*, 2014, **43**, 4563-4601.
5. S. Xu and H. Lu, *Chemical Communications*, 2015, **51**, 3200-3203.
6. L.-K. Zhang, G.-F. Wu, Y. Zhang, Y.-C. Tian, Q.-X. Tong and D. Li, *RSC Advances*, 2013, **3**, 21409-21412.
7. J. Wang, W. Lin and W. Li, *Biomaterials*, 2013, **34**, 7429-7436.

RSC Advances Accepted Manuscript

8. H. Chen, W. Lin, W. Jiang, B. Dong, H. Cui and Y. Tang, *Chemical Communications*, 2015, **51**, 6968-6971.

9. Probes based on the excimer fluorescence have been reported; see references 10 and 11

10. J. Zheng, J. Li, Y. Jiang, J. Jin, K. Wang, R. Yang and W. Tan, *Analytical Chemistry*, 2011, **83**, 6586-6592.

11. C. Wu, L. Yan, C. Wang, H. Lin, C. Wang, X. Chen and C. J. Yang, *Biosensors and Bioelectronics*, 2010, **25**, 2232-2237.

12. S. González-Carrero, M. de la Guardia, R. E. Galian and J. Pérez-Prieto, *ChemistryOpen*, 2014, **3**, 199-205.

13. C. E. Agudelo-Morales, R. E. Galian and J. Pérez-Prieto, *Analytical Chemistry*, 2012, **84**, 8083-8087.

14. W. R. Collin, G. Serrano, L. K. Wright, H. Chang, N. Nuñovero and E. T. Zellers, *Analytical Chemistry*, 2013, **86**, 655-663.

15. Y. Salinas, R. Martinez-Manez, M. D. Marcos, F. Sancenon, A. M. Costero, M. Parra and S. Gil, *Chemical Society Reviews*, 2012, **41**, 1261-1296.

16. M. E. Germain and M. J. Knapp, *Chem Soc Rev*, 2009, **38**, 2543-2555.

17. M. S. Meaney and V. L. McGuffin, *Analytica Chimica Acta*, 2008, **610**, 57-67.

18. B. Balan, C. Vijayakumar, M. Tsuji, A. Saeki and S. Seki, *The Journal of Physical Chemistry B*, 2012, **116**, 10371-10378.

19. K. K. Kartha, S. S. Babu, S. Srinivasan and A. Ajayaghosh, *Journal of the American Chemical Society*, 2012, **134**, 4834-4841.

20. S.-R. Zhang, D.-Y. Du, J.-S. Qin, S.-J. Bao, S.-L. Li, W.-W. He, Y.-Q. Lan, P. Shen and Z.-M. Su, *Chemistry – A European Journal*, 2014, **20**, 3589-3594.

21. Y. Salinas, A. Agostini, E. Perez-Esteve, R. Martinez-Manez, F. Sancenon, M. Dolores Marcos, J. Soto, A. M. Costero, S. Gil, M. Parra and P. Amoros, *Journal of Materials Chemistry A*, 2013, **1**, 3561-3564.

22. W. W. Yu, L. Qu, W. Guo and X. Peng, *Chemistry of Materials*, 2003, **15**, 2854-2860.

23. J. Aguilera-Sigalat, S. Rocton, J. F. Sanchez-Royo, R. E. Galian and J. Perez-Prieto, *RSC Advances*, 2012, **2**, 1632-1638.

24. J. Pérez-Prieto, *Photochemistry and Photobiology*, 2013, **89**, 1291-1298.

25. J. Aguilera-Sigalat, V. F. Pais, A. Doménech-Carbó, U. Pischel, R. E. Galian and J. Pérez-Prieto, *The Journal of Physical Chemistry C*, 2013, **117**, 7365-7375.

26. B.-K. Pong, B. L. Trout and J.-Y. Lee, *Langmuir*, 2008, **24**, 5270-5276.

27. M. Kubista, R. Sjoback, S. Eriksson and B. Albinsson, *Analyst*, 1994, **119**, 417-419.

28. I. E. Borissevitch, *Journal of Luminescence*, 1999, **81**, 219-224.

29. Quantification of TNT in muti-analyte detection (B. C. Giordano, C. Lindsay, K. Johnson Giordano, B. C., Lindsay, C., & Johnson, K. (2014). Chemometric Deconvolution of Continuous Electrokinetic Injection Micellar Electrokinetic Chromatography Data for the Quantitation of Trinitrotoluene in Mixtures of Other NACs (No. NRL/MR/6110--14-9521). NAVAL RESEARCH LAB WASHINGTON DC.

30. R. Polsky, C. L. Stork, D. R. Wheeler, W. A. Steen, J. C. Harper, C. M. Washburn and S. M. Brozik, *Electroanalysis*, 2009, **21**, 550-556.